Assesing of crushing in granular materials using acoustic emission

Caicedo B. & Martinez A.
Department of Civil and Environmental Engineering, Universidad de Los Andes, Bogotá, Colombia
Vallejo L.
Department of Civil and Environmental Engineering, University of Pittsburgh, Pittsburgh PA 15261, USA.

2011 Pan-Am CGS Geotechnical Conference

ABSTRACT
Granular materials experience abrasion and crushing as a result of static or dynamic loads. Despite of the research that has been conducted to date on how to evaluate abrasion and crushing, most of the experimental techniques to evaluate crushing are based on destructive measurements. In this paper the Acoustic Emission technique is used as a tool to asses crushing in a non destructive way.

RESUMEN
Los materiales granulares sufren abrasión o fracturamiento cuando se los somete a esfuerzos estáticos o dinámicos. A pesar de la numerosa investigación en este campo, la mayoría de métodos de evaluación del fracturamiento están basados en técnicas destructivas. En este artículo la técnica de emisiones acústicas se presenta como una herramienta de evaluación no desstructiva del fracturamiento.

1 INTRODUCTION

Granular materials forming part of geotechnical structures like flexible pavements or embankments experience abrasion and crushing as a result of static and dynamic loads applied during the compaction process or during operation. Abrasion takes place when the sharp corners of the particles of gravel are removed as a result of compressive and shear loads. As a result of abrasion the particles change in shape. Crushing is caused by the fragmentation of particles as a result of compressive and shear forces.

Huge research efforts have been conducted on how to evaluate abrasion and crushing and what effect they will have on the engineering properties of granular materials. However most of the experimental techniques to evaluate crushing are based on destructive measurements made after testing. In this study, the abrasion and crushing of sands are evaluated using the acoustic emission technique that is fundamentally a non destructive technique.

The laboratory component of this study involves unsaturated gravels that were subjected to abrasion and crushing by static compression tests.

During the tests the acoustic emission behavior: hits, counts, energy, and duration, are measured as a function of the compression stress; afterwards the measure of the changes in grain size distribution was made. The relationships between mechanical and acoustical behavior are highlighted.

The results show that there is a close relationship between the acoustic emission and the development of plastic strains. Also the results show that the acoustic emission in granular materials is the results of both: sliding between particles, and crushing. Different criteria are applied to the amplitude and duration of the acoustical hits to separate the cause of each emission. As a result different criteria to identify the abrasion and crushing of granular materials using acoustic emission are suggested.

The results of this study provide a new method to evaluate the abrasion and crushing of granular materials in a non destructive manner.

2 THE ABRASION AND CRUSHING OF GRANULAR MATERIALS

Granular materials form part of engineering structures such the base of flexible pavements, highway embankments, and foundations are subjected during their engineering lives to either static or dynamic loads. As a result of the loads, particle abrasion and particle breakage occur (Lee and Farhoomand, 1967; Hardin, 1985; Hagerty et al., 1993; Lade et al., 1996; Coop, 1999; Bolton, 1999; and Feda, 2002). According to Lee and Farhoomand (1967) and Coop (1999), particle breakage or crushing seems to be a general feature for all granular materials. Grain crushing is influenced by grain angularity, grain size, uniformity of gradation, low particle strength, high porosity, and by the stress level and anisotropy (Bohac et al., 2001).

According to Lee and Farhoomand (1967), one of the most important factors influencing the crushing of a mass of granular materials is the crushing resistance of the grains. Coarse granitic sand particles with an average diameter of 2.8 mm have experienced breakage at pressures equal to 2 MPa, while calcareous shells begin crushing at 0.05 to 0.2 MPa (Lade and Farhoomand, 1967, Bohac et al, 2001). Angular particles of freshly quarried materials undergo fragmentation under ordinary pressures (about 0.98 MPa) due to breakdown of sharp angularities (Ramamurthy, 1968). When a granular mass is subjected to a compressive load, the particles resist the load through a series of contacts between the grains. The particles with highly loaded contacts are usually aligned in chains (Cundall and Strack, 1979). Crushing starts when these highly loaded particles fail and break into smaller pieces that move into the voids of the original material. This migration causes the settlement of a granular assembly (Figure 1). Also, on crushing, fines are produced and the grain size distribution curve becomes less steep. Consequently, with continuing crushing, the granular material becomes less permeable and more resistant to crushing. Grain size distribution is a suitable measure of the extent of crushing (Hardin, 1985; Lade et al., 1996).

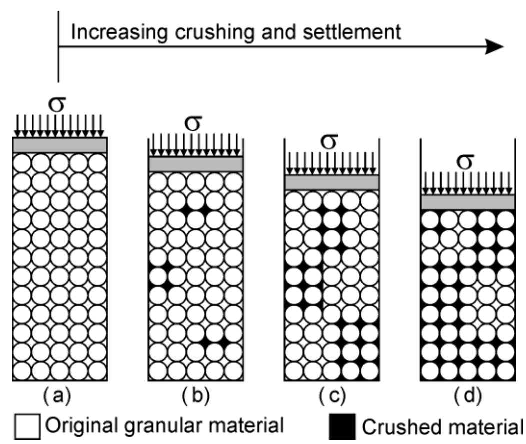

Figure 1. Evolution of crushing in a confined granular material under compression, Vallejo et al. (2004)

Lade et al. (1996) found that if a uniform granular material is crushed, the resulting grain size distribution approaches that of a well graded soil for very large compressive loads. Bolton (1999), and McDowell et al. (1996) established that the grain size distribution of a granular assembly that has been crushed under large compressive loads is a fractal distribution. A well graded particle distribution or a fractal distribution represents a granular structure that is made of grains of all sizes including the original unbroken grains.

The original large grains do not break based on the fact that with more small size particles surrounding them, the average contact stress acting on these large grains tends to decrease (Lade et al., 1996). However, before the granular structure reaches a well graded or a fractal particle size distribution, the granular structure will experience gradual changes in particle sizes depending on the magnitude of the compressive load applied to it.

Pavements are the most unusual structures designed by civil engineers. Water enters through their tops, bottoms, and sides, but because pavements are relatively flat, the water flows out again very slowly unless they are well drained under their full width (Cedergreen, 1994). The most serious problems occur in flexible pavements when their granular bases are unable to remove the water that enters the pavement. Figure 1(a) represents a well drained granular base assuming drainage goes vertically or laterally. In Figure 1(b) the loose zones that drains the water are interconnected (the dense zones filled with crushed material are not connected). Thus, drainage in the vertical or horizontal direction is still possible. In Figure 1(b), the dense zones, which are zones that prevent drainage because of being filled with crushed material, are isolated and not continuous; for that reason drainage is still possible. In Figures 1(c) and 1(d), the loose zones that drain the granular base in either the vertical or horizontal direction are no longer connected. These loose zones must be interconnected in order for water to drain from underneath the pavement. In Figures 1(c) and 1(d), the dense zones made of crushed material are the ones that are interconnected. The dense zones made of crushed granular material surround and isolate the loose zones that promoted drainage.

Thus, when the granular base reaches the conditions of Figures 1(c) and 1(d) as a result of crushing, serious problems will develop in pavements.

Very little is known about non destructive methods to evaluate crushing of granular materials. In this paper the acoustic emission technique is presented as a new experimental technique to assess the level of crushing of such materials.

3 PRINCIPLES OF THE ACOUSTIC EMISSION TECHNIQUE

Mechanical processes like fracture propagation or slipping creates acoustic emission that propagates within a solid body. The acoustic waves propagate to the surface of the body in a similar manner than the earthquake waves traveling through the interior of the earth. The Acoustic Emission method (AE method) is based on the measure at the surface of the body of the waves generated by the mechanical processes.

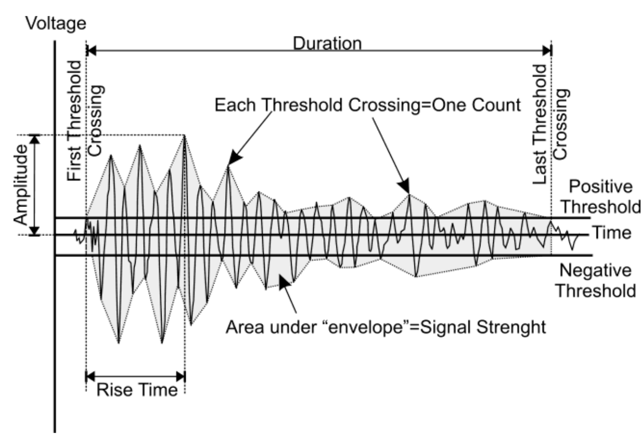

Figure 2. Typical AE signal and AE parameters.

The traditional AE method only captures certain parameters (sometimes called AE features), including AE counts, peak levels, and energies. Then, the AE features are correlated with the defect formation and failures.

Figure 2 shows some typical output from an AE sensor, Berkowitz (1998). When a stress wave strikes the face of the sensor, it causes the output signal to rise above a preset threshold. This signal is commonly referred to as a “hit”. The threshold value will vary depending on the type of data required, and the circumstances of the test. It is used to selectively reject signals with amplitude below the threshold which will not provide meaningful data, as they may be caused by spurious sources such as ambient, electronic, or electromagnetic noise.

Acoustic emission has been observed to occur in bursts, which manifests itself as a number of separate hits within a short period of time. The cascade of hits is useful to characterize the different types of defects. As in earthquakes, the early hits are small in magnitude as premonitory events, afterwards the main energy is released and finally hits occurring at the end of the signal are aftershocks.

3.1 Acoustic Emission parameters

When the AE transducer senses a signal over a certain level (i.e., the threshold), an AE event is captured. The amplitude of the event is defined at the peak of the signal (Figure 2). The number of times the signal rises and crosses the threshold is the count of the AE event. The time period between the rising edge of the first count and the falling edge of the last count is the duration of the AE event. The time period between the rising edge of the first count and the peak of the AE event is called the rise time. The area under the envelope of the AE event is the energy or strength of the signal.

Other AE parameters are used to understand the processes occurring during mechanical loading. Signal strength and amplitude are typically used together to provide a measure of the magnitude of typical events, such as yielding and crack propagation.

The Kaiser effect is a powerful and important tool in the evaluation of acoustic emission data. The effect is defined as follows: if a material is stressed and monitored with AE, the stresses removed, and then reapplied, no acoustic emission occurs until the load reaches the level corresponding to the maximum load in the previous stage.

The Felicity effect is the breakdown of the Kaiser effect. The Felicity ratio is defined as the ratio between the load at the onset of acoustic emission during a reload test and the maximum load applied to the element during the previous loading interval. In metals it has been shown that the Felicity ratio is related to the degree of deterioration or damage of the element. A value very close to unity is characteristic of a material in good health, while smaller values (less than 1) are representative of the fact that damage has occurred.

Figure 3 presents the Kaiser and Felicity effect, as obtained from a typical test. In this figure, the Kaiser effect may be noted in the second loading stage. The emission continues just as the load reaches the maximum value attained at the end of the first loading.

The Felicity effect can be seen in the third loading, since the emission starts before the load reached the maximum value of the previous loading. For this case, the Felicity ratio is P2/P1.

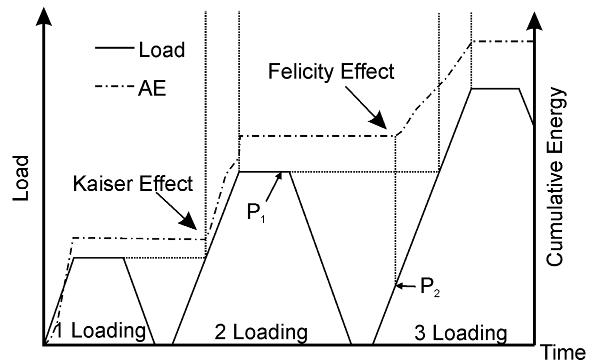

Figure 3. Kaiser and Felicity effects, Berkowitz (1998).

3.2 Filtering criteria

Some AE could be false emissions related to mechanical vibrations, movement of the cables and sensors, etc. Also false emissions due to sliding friction are a particular problem with the setup used in the laboratory Berkowitz (1998).

Some techniques have been developed for identifying false emission and applying post-test filtering. Filters, such as the Swansong filters (Berkowitz 1998), eliminate spurious emission from the data record.

For example the Swansong II filter is conceived to eliminate mechanical sliding. This filter is based on linking certain hit parameters such as low amplitude and long duration with sliding. With this filter the data are removed for a period of 1 second when the following conditions become noticeable:

$$\text{If } (A_i - A_{th}) < 5 \quad \text{and} \quad D_i > 2 \qquad [1]$$
$$\text{or } (A_i - A_{th}) < 10 \quad \text{and} \quad D_i > 3.5$$
$$\text{or } (A_i - A_{th}) < 15 \quad \text{and} \quad D_i > 4.5$$

Under these conditions all hits during the period (Ti-0.5) to (Ti+0.5) in seconds are eliminated. In previous equations, Ai is the amplitude in dB, Ath is the data acquisition threshold in dB, Di is the hit duration in ms, and Ti is the arrival time in sec.

3.3 Intensity analysis

Another important technique in the evaluation of AE data is the Intensity analysis. The two basic parameters used for this analysis are the Severity Index and the Historic Index. Intensity analysis is a measure of the structural significance of an acoustic emission source. The technique has been used extensively for analysis of defects in metal equipment, Fowler et al. (1989). However, nowadays this technique is useful only for metals since it is based on test data from destructive tests and controlled tests with detailed follow-up non-destructive evaluation.

Intensity analysis uses two factors based on signal strength. The first factor is known as historic index, and compared the signal strength of the most recent hits to the signal strength of all hits. The second factor, referred to as severity, is the average of the largest signal strength hits striking the sensor. Historic index H(t), and severity, Sr are defined as follows:

$$H(t) = \frac{N}{N-K}\left(\frac{\sum_{t=K+1}^{N} S_{0i}}{\sum_{i=1}^{N} S_{0i}}\right) \qquad [2]$$

$$S_r = \frac{H_f}{J}\sum_{m=1}^{m=J}\psi(h)S_{0_m} \qquad [3]$$

Where: N is the number of hits up to and including time t, S0i is the signal strength of the ith hit, K is an empirically derived factor, S0m is the signal strength of the mth hit (being ordered on the magnitude of the signal strength), J is an empirically derived constant that depends on the material, Hf is known as the Maize factor and depends on the loading, and □(h) is a function of the threshold.

In common AE test for metals, the results of the intensity analysis are plotted on a chart divided into zones which shows the structure mechanical condition.

3.4 Acoustic Emission in Geotechnics

Acoustic emission techniques have been used in rock mechanics to assess the stability of mines, Ober (1941). Koerner et al. (1974 and 1976) include AE devices in triaxial and oedometer apparatus to test silty and sandy samples; these studies highlight the ability of AE to identify plastic strains. The capability of AE to recognize plastic strains has been confirmed by Tanimoto et al. (1981), Tanimoto and Nakamura (1981), Tanimoto and Tanaka (1986 and 1988), and Tanaka (1999).

4 MATERIAL AND METHODS

4.1 Experimental set up

Figure 4 presents a typical AE system setup. The AE transducers are generally very sensitive piezoelectric sensors. Because the traditional AE technique only uses AE features, the actual waveforms are not critical to this method. The AE sensors used are usually resonance sensors, which are only very sensitive to a certain frequency. Since the AE signals are very weak, a preamplifier is connected right after the AE transducer to minimize the noise interference and prevent the signal loss. Then, the signals pass through a filter to remove the noise. The signals are amplified by the main amplifier before being sent to the signal conditioner. After that, the AE features are stored in a computer for further analysis. During investigations, other parameters, such as load, deformation, pressure, and temperature, can also be recorded as parametric inputs.

For this study the sample is confined in a cylindrical mould having 150 mm diameter and 150 mm height, the sample is compacted applying vertical stresses using a frame with 100 kN capacity. The loading apparatus is equipped with a load cell and a displacement transducer type LVDT (Figure 5a).

The sides of the cylindrical mould were lubricated to reduce the friction. The AE sensor is located at the base of the mould as shown in Figure 5(b) and 5(c).

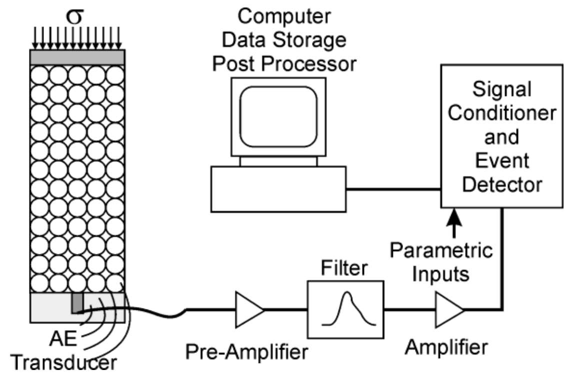

Figure 4. Configuration of the AE system.

The other component of the experimental setup is the acoustic system that is made up of a PCI card having an 18 bit A/D converter, a preamplifier and a piezoelectric sensor. The PCI card has the following features: bandwidth of 1 kHz to 3 MHz, sampling frequency 40 MHz, 4 high pass and 6 low pass filters; the preamplifier have possibility of apply three gains 20, 40 and 60 dB.

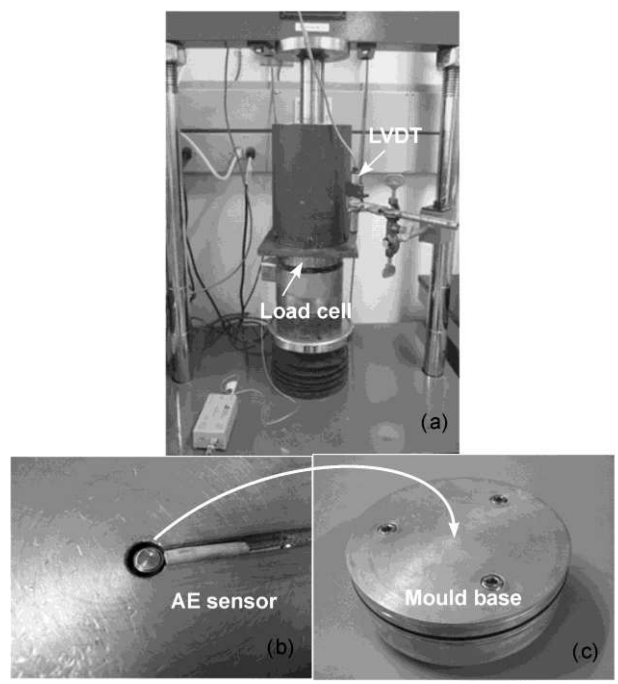

Figure 5. Experimental setup..

The tests were performed with the following settings: threshold 34 dB, bandwidth 20-200 kHz, sampling frequency 1 Msample/s, and pre amplifier at 20 dB.

4.2 Experimental set up

Compression tests were carried out on a Vista Hermosa granular material that is used frequently as granular base for pavements in Bogotá Colombia. Properties of this material are summarized in Table 1.

Table 1. Properties of Vista Hermosa Material

I_p %	D_{max} (mm)	LA %	C_u	C_c
9	25.4	20	12.3	1.3

I_p: plasticity index; D_{max}: maximum grain size; LA: Los Angeles abrasion tests; C_u: uniformity coefficient; C_c curvature coefficient.

Granular material was prepared at three different water contents (2.7%, 4.1%, and 5.4%), afterwards compression tests with three loading and two unloading stages were performed. The final stresses during these loading-unloading cycles are presented in Table 2.

Table 2. Stresses during loading-unloading stages

Stage	Stress kPa
First loading	1000
First unloading	300
Second loading	2300
Second unloading	800
Third loading	4500

5 RESULTS AND ANALYSIS

Figure 6 shows the evolution of stress and strain during compression tests as well as the AE response represented as the growth of cumulated hits and cumulated absolute energy. In these figures the Kaiser and Felicity effects are easily noticeable; during the first loading-unloading stage the Felicity ratio is 1 although during the second cycle this ratio reduces to 0.86. This reduction on the Felicity ratio indicates that the increase of acoustic events initiate before reaching the maximum stress achieved during the loading stage. As acoustic events could be related to plastic strains, the reduction of the Felicity ratio indicates that some plastic strains appear before the maximum previous stress.

Figure 7 shows the relationship between stress and strain as well as stress and cumulated hits. During the first loading stage there are significant plastic strains although there is a few number of hits. As during this first loading the sample experiences relatively low stresses, most of the hits registered during this stage could be related with slides between particles. During the second loading stage the slope of the curve of stresses and strains becomes slightly steeper than during the first loading cycle and the number of hits increases significantly. As during the second and third loading cycles the sample experiences high stresses, this appreciable increase of the number of hits could be associated with crushing.

The change of the grain size distribution after loading is presented in Figure 8, it is noticeable that the three samples undergo the same level of crushing although the plastic strain and the number of hits are different for each water content (Figure 7). This comparison indicates that AE registers sliding of particles and crushing at the same time. An idea of a method to discriminate sliding and crushing could be obtained analyzing the other AE features.

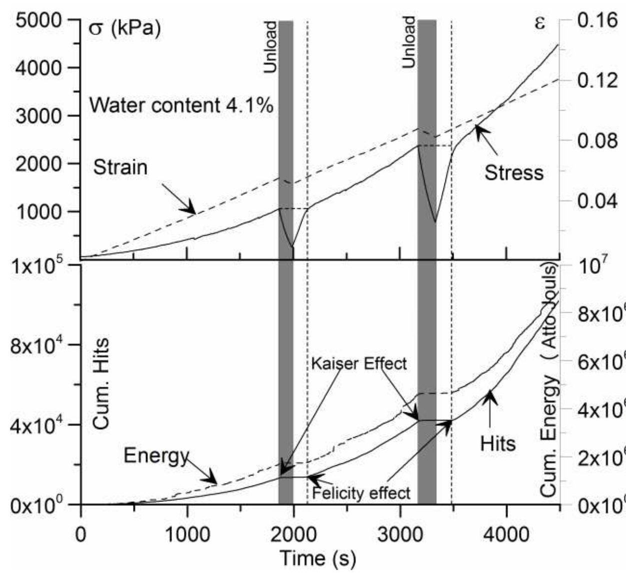

Figure 6. Stress, strain and AE features during loading and unloading, water content w=4.1%.

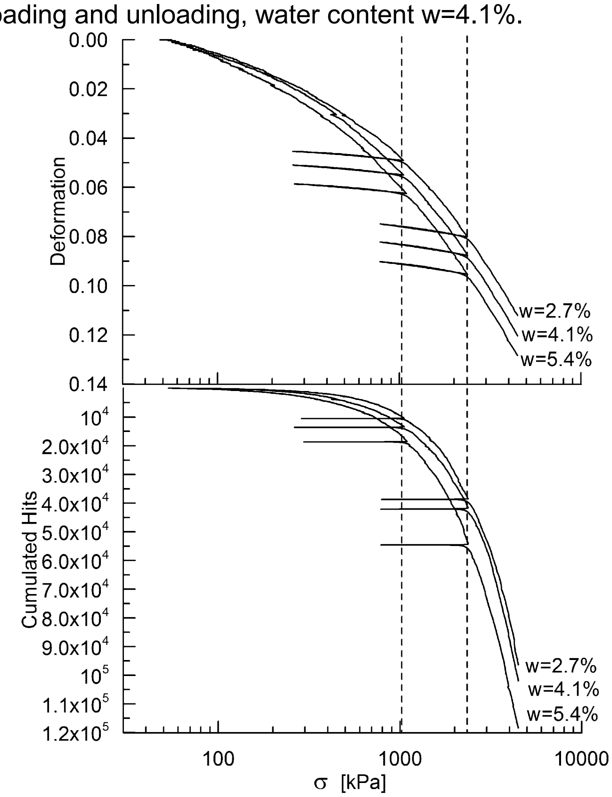

Figure 7. Strain stress and cumulated hits registered during the loading and unloading cycles for the three water contents.

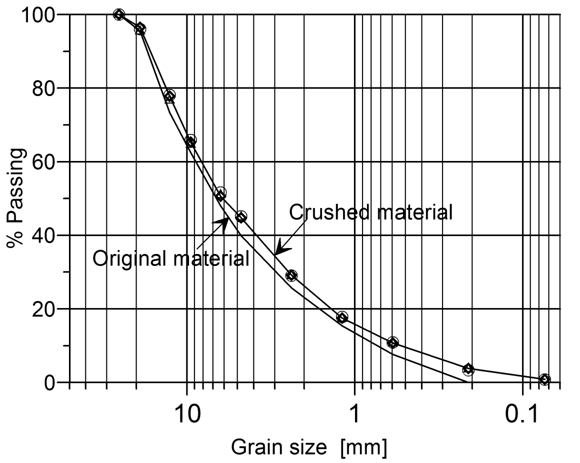

Figure 8. Grain size distribution before and after loading.

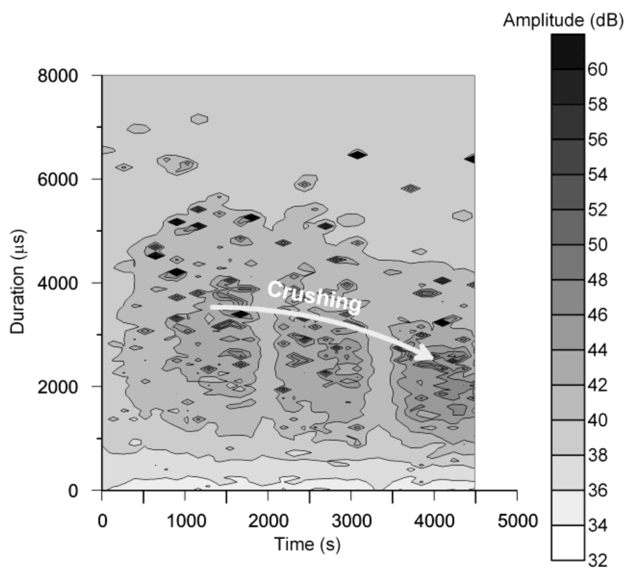

Figure 9. Duration and amplitude of the hits during the loading and unloading stages, water content w=4.1%.

The Swansong filter gives an idea of the AE features that have to be analyzed to discriminate sliding. In fact, this filter is based on the assumption that long and weak hits could be associated to sliding while short and strong hits represent propagation of cracks in the material. Figure 9 shows the duration and amplitude of the hits during loading and unloading, this figure indicates that during the second and third cycle there is higher number of hits in the short and strong region compared with the first loading stage.

Another possibility to discriminate hits due to crushing is to analyze other AE features like counts to peak and total number of counts in each hit, as well as the rise time and duration of each hit. In fact as the crushing is the result of energy accumulation within particles, it is expected that the hits due to crushing could appear without significant premonitory counts. If it is true, the relationship between counts to peak to total number of counts in each hit could be lower for hits due to crushing than hits due to sliding; this judgment is also valid for the relationship between rise time and duration of each hit. These two relationships are presented in Figure 10, this figure shows higher concentration of hits for low values of the previously described relationships during the second and third loading stages.

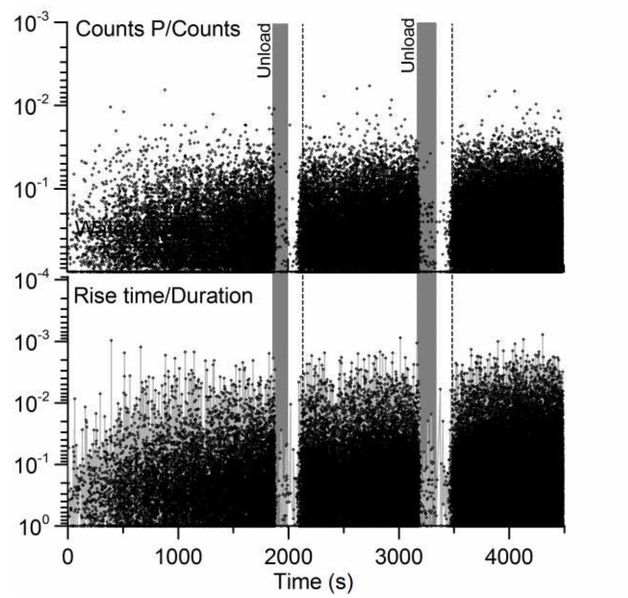

Figure 10. Relationship between counts to peak and total counts, and rise time and duration, w=4.1%.

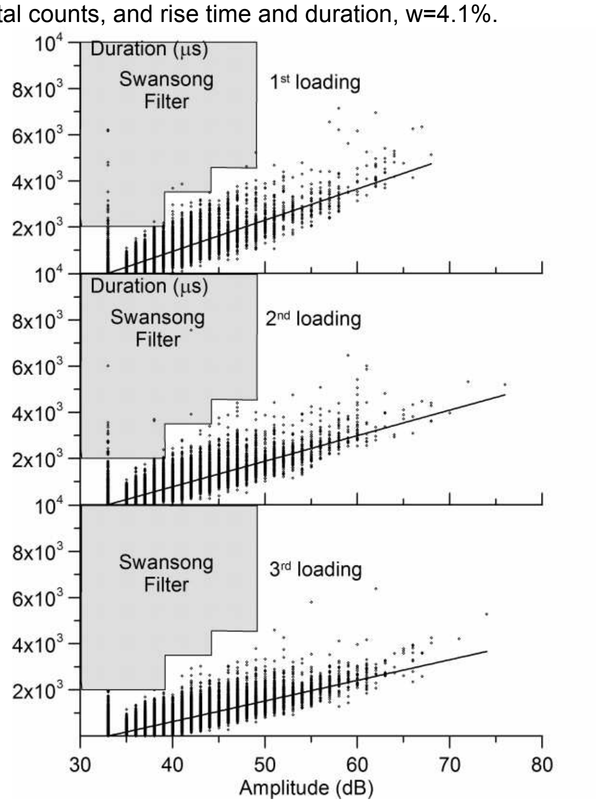

Figure 11. Hit duration and amplitude w=4.1%.

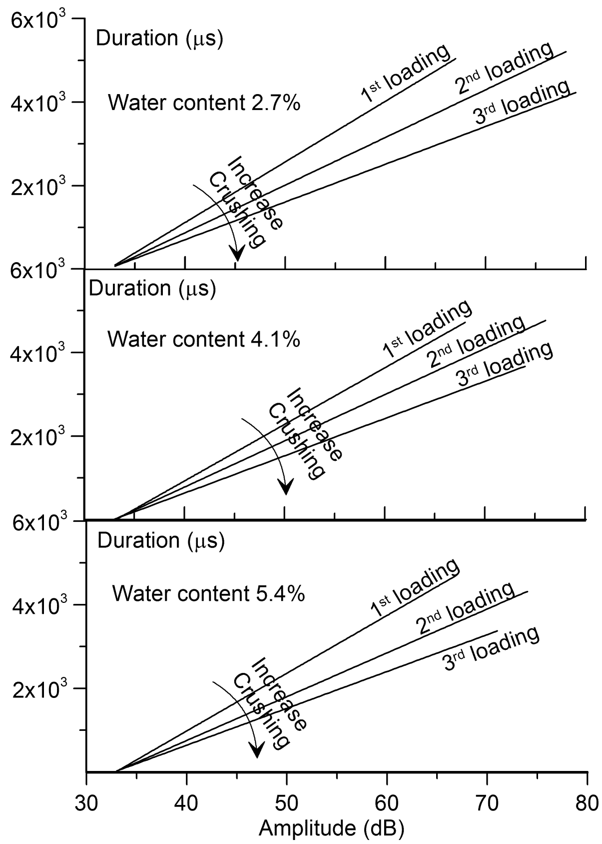

Figure 12. Linear relationship between hit duration and amplitude for each water content.

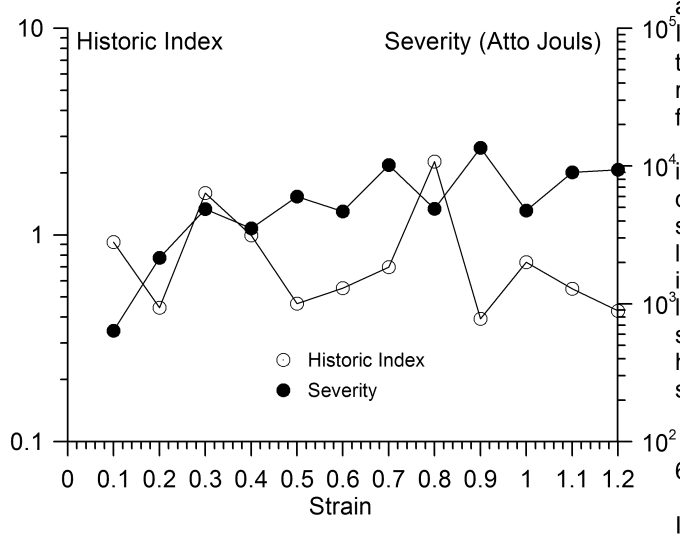

Figure 13. Evolution of historic index and severity with strain, water content w=4.1%.

Figure 11 shows the relationship between hit duration and amplitude for each loading cycle, the Swansong Filter is represented in this figure as well. The results on granular materials reveal that only few hits fall in the Swansong Filter region, this means that most of the hits originated by the mechanical movement of the whole experimental setup are rejected using threshold of 34 dB. Figure 11 shows also the linear relationship between duration and amplitude, the slope of this relationship reduces for higher compressive stresses and therefore for higher level of crushing. Figure 12 shows the linear relationship for each loading stage and for each water content, as observed for the three water contents the slope reduces for higher stresses; as a consequence the slope of the relationship Duration/Amplitude could be a good indicator of the level of crushing.

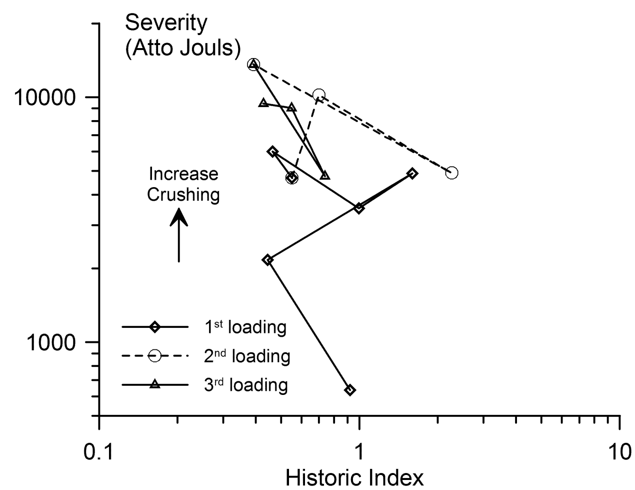

Figure 14. Historic index and severity for the different loading cycles, water content w=4.1%.

Another possibility to analyze crushing is performing an intensity analysis. Figures 13 and 14 show the Historic Index and Severity calculated using equations 2 and 3. In this equations, parameters K, J, H_f, and $\psi(h)$ are respectively 200, 50, 1, and 1 as used by Lovejoy (2008) for concrete structures.

Figure 13 shows the increase of severity as the strain increases, however the variation of the historic index doesn't show any clear relationship with strain. Figure 14 show a plot of severity and historic index for the three loading stages, in this plot it is clearly noticeable the increase of severity as the stress grows and then the level of crushing increases. This analysis suggests that severity of the AE could be a good indicator of crushing, however more tests are required to confirm this statement.

6 CONCLUSIONS

In this paper the possibility of assess crushing of granular materials using a non destructive technique like acoustic emission is analyzed. The result shows that acoustic emission is affected not only by the breakage of particles but also by sliding. For this reason to assess crushing using AE it is necessary to use some criteria based on the analysis of the AE features. The relationship between the duration and amplitude of each hit as well as the evolution of severity during loading are promising tools to discriminate hits due to breakage and sliding. However more tests on materials having different degree of crushing are required to confirm this preliminary estimate.

REFERENCES

Berkowitz, P., C., (1998). “Crack Detection in Crane Shafts Using Acoustic Emission”. Msc. Thesis The University of Texas at Austin, May 1998.

Bohac, J., Feda, J., and Kuthan, B., 2001. “Modelling of grain crushing and debonding”. Proceedings of 15th Int. Conference on Soil Mech. And Geotech. Eng., Istanbul, Turkey, Vol. 1, pp. 43-46.

Bolton, M.R., 1999. “The role of micro-mechanics in soil mechanics”. Proceedings of the Int. Workshop on Soil Crushability, Yamaguchi, Japan, pp. 58-82.

Cedergren, H.R., 1994. “America’s pavements: world’s longest bathtubs”. Civil Engineering, September, pp. 56-58.

Coop, M.R., 1999. “The influence of particle breakage and state on the behavior of sands”. Proceedings of the Int. Worshop on Soil Crushability, Yamaguchi, Japan, pp. 19-57.

Cundall, P.A., and Strack, O.D.L., 1979. “A discrete numerical model for granular Assemblies”. Geotechnique, Vol. 29, No. 1, pp. 47-65.

Feda, J., 2002. “Notes on the effect of grain crushing on the granular soil behaviour”. Engineering Geology, Vol. 63, No. 2, pp. 93-98.

Fowler, T.J., J.A. Blessing, P.J. Conlisk, and T.L. Swanson, “The MONPAC System,” Journal of Acoustic Emission, Vol. 8, No. 3, 1989.

Hagerty, M.M., Hite, D.R., Ullrich, C.R., and Hagerty, D.J., 1993. “One-dimensional high-pressure compression of granular media”. Journal of Geotechnical Engineering, ASCE, Vol. 199, No. 1, pp. 1-18.

Hardin, B.O., 1985. “Crushing of soil particles”. Journal of Geotechnical Engineering, ASCE, Vol. 110, No. 10, pp. 1177-1192.

Koerner, R.M., Lord A.E., 1974. Acoustic Emission in Stressed Soil Sample. The Journal of the Acoustical Society of America, 56 (6), 192̃41926.

Koerner, R.M., Lord A.E., McCabe, W.M., Curran J.W., 1976. Acoustic Emission Behavior of Granular Soils. Journal of the Geotechnical Engineering Division, 102(7), 76̃1773.

Lade, P.V., Yamamuro, J.A., and Bopp, P.A., 1996. “Significance of particle crushing in granular materials”. J. of Geotechnical Eng., ASCE, Vol. 122, No. 4, pp. 309-316.

Lee, K.L., and Farhoomand, J., 1967. “Compressibility and crushing of granular soils in anisotropic triaxial compression”. Canadian Geotechnical J., Vol. 4, No. 1, pp. 68-86.

Lovejoy S., C., (2008). Acoustic emission testing of in-service conventionally reinforced concrete deck girder superstructures on highway bridges. Report SPR 633, Oregon Department of Transportation, 30 p.

McDowell,G.R., Bolton, M.D., and Robertson, D., 1996. “The fractal crushing of granular materials”. Int. J. of Mechanics and Physics of Solids, Vol. 44, No. 12, pp. 2079-2102.

Obert, L., 1941. Use of subaudible noises for prediction of rockbursts. US Bureau of Mines Report 3555.

Ramamurthy, T., 1968. “Crushing phenomena in granular soils”. The Journal of the Indian National Society of Soil Mech. and Found. Eng., Vol.8, No. 1, pp. 67-86.

Tanaka, Y., 1999. Use of Acoustic Emission to Detect Yield Point. Oda, M., Iwashita, K., Mechanics of Granular Materials. An Introduction. Balkema, 270̃276.

Tanimoto, K., Tanaka, Y., 1988. Time Dependent Deformation of Sand Measured by Acoustic Emission. Proc. International Conference on Rheology and Soil Mechanics, 12̃16.

Tanimoto, K., Tanaka, Y., 1986. Yielding of Soil as Determined by Acoustic Emission. Soils and Foundations, 26(3), 69̃80.

Tanimoto, K., Nakamura, J., 1981. Studies of Acoustic Emission in Soils. Acoustic, Emission in Geotechnical Engineering Practice, ASTM 750, 164̃173.

Vallejo, L.E., Chik, Z., Tucek, S., and Caicedo, B. (2004). Fractal analysis of the abrasion and crushing of gravels. Proceedings of the 6th Int. Conf. on Pavements Unbound, Nottingham, England, Dawson, A.R. (ed.), A.A. Balkema Publishers, pp. 43-50.